SiliconPV 2024, 14th International Conference on Crystalline Silicon Photovoltaics
Module Technologies
https://doi.org/10.52825/siliconpv.v2i.1407
© Authors. This work is licensed under a Creative Commons Attribution 4.0 International License
Published: 09 Jan. 2025

Characterization of Electrically Conductive Adhesives to Enable Perovskite-Silicon Tandem Solar Cell Interconnection

Leonhard Böck[1,2] and Torsten Rößler[2]

[1] Fraunhofer Institute for Solar Energy Systems, Germany

[2] Karlsruhe Institute for Technology, Germany

*Correspondence: Leonhard Böck, leonhard.boeck@ise.fraunhofer.de

Abstract. The mechanical stability of interconnections in solar modules is crucial for their long-term performance. Electrically conductive adhesives (ECAs) offer a promising solution for the interconnection of perovskite-silicon tandem (PVST) solar cells due to their low-temperature processibility. In this study, the influence of low curing temperatures on the mechanical and electrical properties of ECAs was investigated to assess their suitability for PVST technology. Four commercially available ECAs were characterized, focusing on curing temperatures of 100 °C, 140 °C, and 180 °C. Mechanical characterization through tensile tests and dynamic mechanical analysis (DMA) revealed varying Young's modulus (E) (stiffness) and glass transition temperatures (T_G) among the ECAs. Electrical characterization showed that lower curing temperatures can lead to lower volume resistivity. This was particularly true for ECA C, which is an acrylate-based, highly filled ECA. However, joint resistance values exhibited high standard deviations. Void analysis indicated that void formation had a negligible effect on the mechanical properties of ECAs. Furthermore, the influence of remaining enthalpy after curing, interpreted as the curing degree, on mechanical and electrical properties was investigated. The results highlighted the importance of complete curing for achieving the desired properties. Overall, this study provides valuable insights into optimizing the interconnection process for PVST solar cells, essential for enhancing the long-term stability and performance of solar modules.

Keywords: Electrically Conductive Adhesive (ECA), Perovskite-Silicon-Tandem Solar Cells, Low-Temperature Curing

1. Introduction

The interconnection of perovskite silicon tandem (PVST) solar cells still poses a huge challenge due to the thermal instability of perovskites. Currently available perovskites are incompatible with conventional soldering processes [1]. To fabricate PVST solar modules, new paths must be taken.

Electrically conductive adhesives (ECAs) offer a great solution for the interconnection process due to their low-temperature processibility. ECA-interconnected, highly efficient PVST modules have been demonstrated recently [2].

Extensive research on bulk properties of ECAs [3], [4] and properties in solar cell joints [5] has already been carried out. However, to the authors' knowledge, the influence of perov-

skite compatible, low-temperature curing processes on the properties of ECAs has not yet been studied in detail.

This study aims to investigate the influence of low-temperature curing on:

- **Mechanical properties:** Viscoelastic behaviour, flexibility and cohesion are critical factors for the resilience against mechanical/thermomechanical loads and for string handleability.
- **Electrical properties:** Volume resistivity and contact resistance determine the interconnection losses.
- **Curing degree:** Incomplete curing can have an impact on mechanical and electrical properties and could lead to an undesirable change of joint properties during module lifetime.

2. Materials and Methodology

Tensile tests were used to measure tensile strength (σ_m) and Young's modulus (E) The tensile strength is the limiting factor if static forces, for example due to string handling, lead to cohesive fracture. Using die shear tests, a previous study demonstrated that cohesive properties, rather than adhesive properties, can be the limiting factor for some ECAs [6].

Young's modulus E is an important parameter for the resilience against thermomechanical loads. Especially for shingled solar cells, a low modulus is required to compensate thermomechanical loads [7]. Also for ribbon interconnection, a lower modulus could be beneficial to compensate the different thermal expansions of silicon (solar cell) and copper (ribbon/wire).

To describe the viscoelastic behaviour, the glass transition temperature T_G was measured using dynamic mechanical analysis (DMA). At T_G, polymers transform from a hard, glassy state, to a soft, rubbery state. Below T_G, elastic properties are dominating. Above T_G, both viscous and elastic properties are significant. For PV applications, it is desirable that T_G is outside of the operating temperature range, so that the interconnection properties are independent from the season.

Electrical properties, as volume resistivity and joint resistance, determine the interconnection losses and were characterized using a simple model geometry.

To determine the curing degree, bulk ECA samples were cured in a lamination-like process, which were then put in differential scanning calorimetry (DSC) to measure the remaining reaction potential.

2.1 Selection of ECAs and curing temperatures

ECAs for solar cell interconnections are available with a wide spectrum of formulations, resulting in different curing processibilities, as well as different mechanical and electrical properties. To cover the broad spectrum of typical ECAs, four commercially available ECAs with a broad range of physical properties (base polymer, flexibility, and filler content) were selected for the study. Relevant data sheet values are listed in Table 1. A more flexible material has a lower modulus. The density of ECAs correlates with filler content due to the high density of metallic filler particles.

Table 1. *Data sheet values of the selected ECAs*

ECA	Polymer	Modulus at RT (MPa)	Density (g/cm³)
ECA A	Epoxy	175	4.2
ECA B	Epoxy	1200	3.0
ECA C	Acrylate	2600	4.4
ECA D	Epoxy	No value given	2.0

As curing temperatures (T_{curing}), 100 °C, 140 °C and 180 °C were chosen for the study. 100 °C was chosen as lower end temperature for industrial feasibility, 140 °C is an upper temperature limit for some perovskites [1], and 180 °C is a conventional reference temperature.

2.2 Tensile tests

Samples for tensile tests were produced by pouring ECA in a mold, flattening the surface with a squeegee and finally curing in a convection oven for 20 min, to simulate the heat input from a typical encapsulation process. The samples were shaped according to DIN EN 527, type 1BA and 0.3 mm thick.

A ZwickiLine Z0.5TN from Zwick was used. The tests were performed according to ISO 527. The test velocity was 1 mm/min. Seven samples per ECA were produced initially. Groups with the highest scattering were enlarged to ten samples. As some samples broke during preparation, the smallest group consisted of four samples.

2.3 Dynamic mechanical analysis

Dynamic mechanical analysis (DMA) was used to assess the glass transition temperature (T_G). The samples were produced in the same way as samples for tensile tests. The samples had a rectangular cross section, which was 5 mm wide and 0.3 mm thick. Tests were conducted using a Gabo Eplexor 500 N from Netzsch. To prevent sample breakage and slippage in the clamps, low stresses (1.5 MPa (static) and ±1.4 MPa (dynamic)) were used in the test. The frequency of the dynamic load was 1 Hz. The temperature range was chosen from −40 °C to +160 °C. The heating rate was 1 °C/min, as recommended in ISO 6721. Each test was repeated three times.

2.4 Electrical characterization

To assess volume and joint resistance, specially designed, silver-coated printed circuit boards (PCB), as shown in Fig. 1a, were used. The PCB features two types of test structures:

- Silver/ECA/ribbon joints (Fig. 1b) to determine the joint resistance R_{joint}, which was calculated as follows:
$$R_{\text{joint}} = R_{\text{meas}} - R_{\text{ribbon}}$$
Where R_{meas} is the measured total resistance and R_{ribbon} is the resistance of the ribbon. R_{joint} consists of the contact resistances between Ag and ECA, ECA and ribbon and the volume resistance of the ECA
- Pure ECA pads to determine the volume resistivity ρ (Fig. 1c)

ECA was applied to the PCB using manual stencil printing. Ribbons were manually applied and fixed during curing using a spring-loaded downholder. A four-point measurement system (Keithley 2128A/6220) was used to measure resistances. To calculate resistivity, the

geometry of the printed ECA pad was measured using a confocal microscope. A representative 3D image is shown in Fig. 1d.

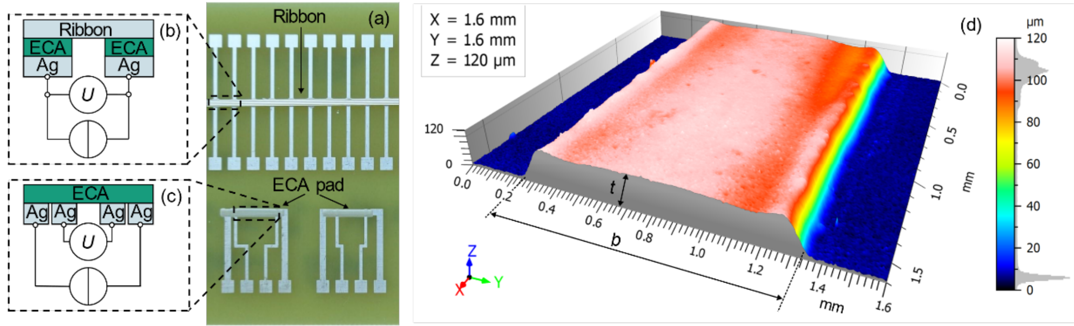

Figure 1. *Setup for the electrical characterization of ECAs. (a) PCB with printed ECA pads and ECA bonded ribbon. Sketch of the measurement setup for (b) joint resistances and (c) resistivities. (d) Geometry of a segment of a cured ECA pad, measured using confocal microscopy*

2.5 Differential scanning calorimetry

To estimate the curing degree, we measured remaining reaction enthalpy *H* using differential scanning calorimetry (DSC) according to DIN EN ISO 11357-5. A Q2500 from TA instruments was used. To determine *H*, ECA samples were cured and stored at ambient atmosphere and temperature for at least two days, to ensure that all post-curing processes are finished. The samples were subjected to two heating/cooling cycles in the DSC. An example measurement is shown in Fig. 2. The crosshatched area shows the difference between the first and second heating cycles. The second cycle behaves linear between 40 °C and 200 °C, indicating that only the heat capacity is measured. *H* was calculated by integrating the difference in heat flow between the first and second cycles over the temperature.

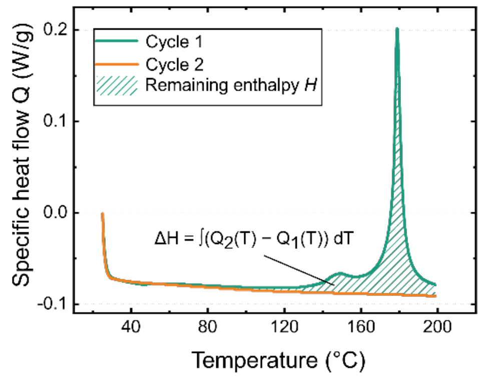

Figure 2. *Measurement of the remaining enthalpy of the sample.*

2.6 Void analysis

To measure void formation, cross-sections of cured samples were prepared. The number and area of voids were measured using microscopic images. A representative image is shown in Fig. 3a. Number and area of the voids were measured via thresholding in ImageJ. A representative evaluated image is shown in Fig. 3b.

(a) ECA sample, Sample fixation
(b) Voids

Figure 3. *Cross section microscopic image (ECA A, 180 °C). (a) unedited microscopic image, (b) edited image. Identified voids are highlighted in red*

The relative void area A_{rel} was calculated as follows:

$$A_{\mathrm{rel}} = \frac{\sum A_{\mathrm{void,i}}}{A_{\mathrm{cross}}}$$

where $A_{\mathrm{void,i}}$ is the area of a single void and A_{cross} is the cross-sectional area of the whole sample.

3. Results and discussion

3.1 Mechanical characterization

In the Young's modulus E obtained from tensile tests (see Fig. 4a), two distinct behaviors are observed: while E from ECA B and C increases with curing temperature, E from ECA A and D is independent of the curing temperature. For ECA B and C, low-temperature curing may be beneficial for long-term joint stability, since lower curing temperatures tend to result in lower E.

The tensile strength of all ECAs (Fig. 4b) exhibits similar behavior as the Young's modulus. Samples of ECA C, cured at 100 °C, were very fragile, many broke during manual handling. All other samples were sufficiently stable for manual handling.

The glass transition temperature T_G from ECA A and B (Fig. 4c) is independent of the curing temperature. Low-temperature cured samples from ECA C failed due to low mechanical stability at high temperatures. The T_G from ECA D is significantly lower when cured at 100 °C.

The glass transition from ECA A occurs around 60 °C. Since cell temperatures in tropical countries can reach this level, the material behavior may transition between glassy and rubbery states during normal module operation [8]. The T_G of ECA B and D is higher than the typical module operating temperatures. This is preferred, as constant material behavior facilitates more accurate lifetime prediction.

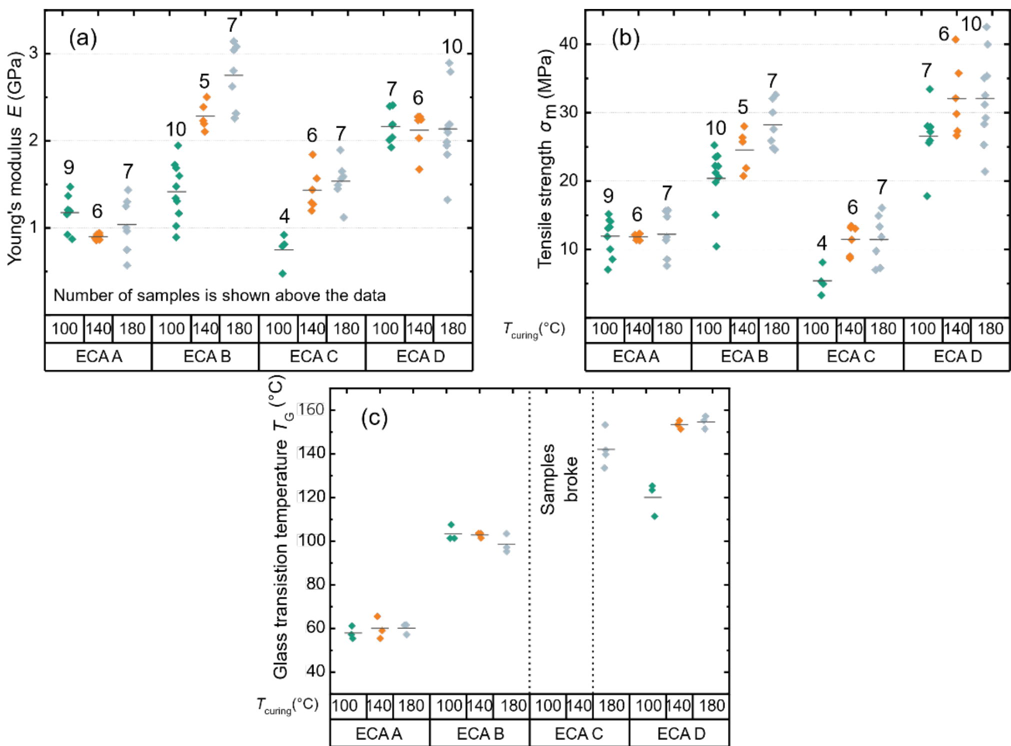

Figure 4. *Results of mechanical ECA characterization. (a) Young's modulus E and (b) tensile strength obtained from tensile tests and (c) glass transition temperature* T_G *obtained from DMA*

3.2 Electrical characterization

The electrical properties of each ECA respond differently to the chosen curing temperature. The volume resistivity of ECA A and B (Fig. 5a) is only minimally influenced, staying within the standard deviation range. In contrast, ECA C and D are clearly affected. For ECA C, volume resistivity decreases with higher curing temperatures. Conversely, ECA D exhibits higher volume resistivity at increased curing temperatures.

The measured joint resistance (Fig. 5b) exhibits high standard deviations. This is mainly caused by the manual sample preparation. For ECA A, B and C, 140 °C appears to be the optimal curing temperature regarding lowest joint resistance. However, the differences between groups are within the standard deviation range and therefore not statistically significant. Future studies should aim to improve and automate the sample preparation to reduce variability and improve the reliability of resistance measurements.

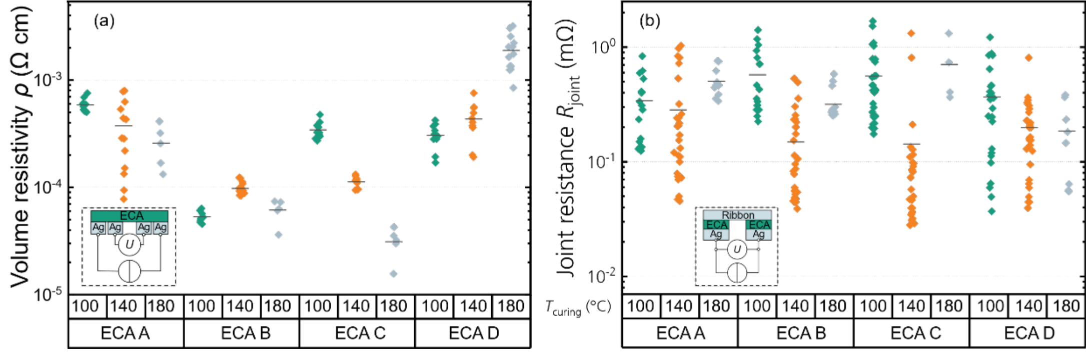

Figure 5. *Results of electrical ECA characterization. (a) volume resistivity and (b) joint resistance*

3.3 Influence of void formation

Studies have shown that temperature-dependent void formation can have an influence on the mechanical properties of ECA joints [6]. It is expected that voids result in reduced stiffness due to the decreased cross-sectional area [9]. To further investigate, cross-sections of bare ECA samples were studied using optical microscopy. Results are shown in Fig. 6. No void formation was observed in ECA C and D. However, in ECA A, no influence is observed, and in ECA B, the stiffness increases with the void area. This suggests that void formation has a lower effect than the curing degree on the mechanical properties of these ECAs.

It was hypothesized that if conductive particles in an ECA agglomerate on void surfaces, the percolation threshold of the material could be lowered, thereby increasing conductivity. However, results indicate that even high voiding degrees (>5%, ECA A, shown in Fig. 6b) do not result in a statistically significant improvement in conductivity. This result has important implications for the design and manufacturing of ECAs, indicating that efforts to control void formation may not be as critical for conductivity.

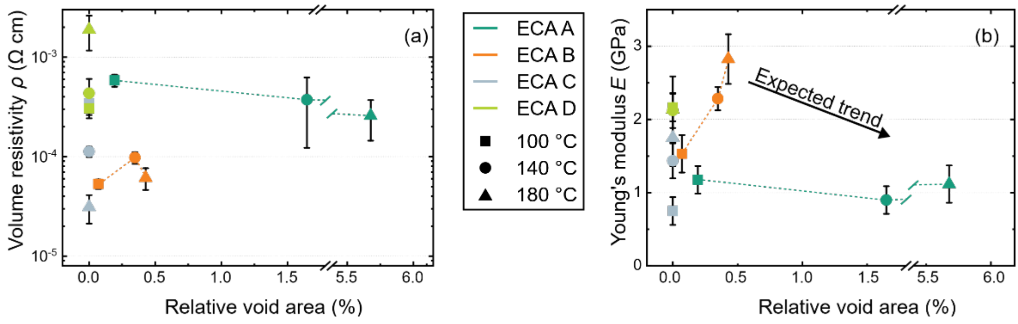

Figure 6. *Mechanical (E) and electrical (ρ) ECA properties in dependence of void formation*

3.4 Influence of the curing degree

Fig. 7 shows the influence of remaining reaction enthalpy H on E (Fig. 7a), and ρ (Fig 7b). All evaluated ECAs are not cured to 100%, when cured at 100 °C. When cured at 140 °C, only ECA A has no remaining enthalpy. Thus, it is the only material in the experiment, which can be fully cured at 140 °C. In ECA B and C, a linear correlation between H and E can be observed. In ECA A and D, incomplete curing seems to play only a minor role for the resulting E.

The remaining enthalpy can also explain the influence of the curing temperature on ρ (Fig. 7b). For ECA C, ρ correlates linearly with H, suggesting that the polymer network formed at low curing temperatures is not stable enough to support high conductivity. Conversely, ρ for ECA D increases with higher curing temperatures. This material uses the capillary suspension principle to lower the percolation threshold [10]. It is likely that the capillary network is damaged by high curing temperatures, leading to higher volume resistivities.

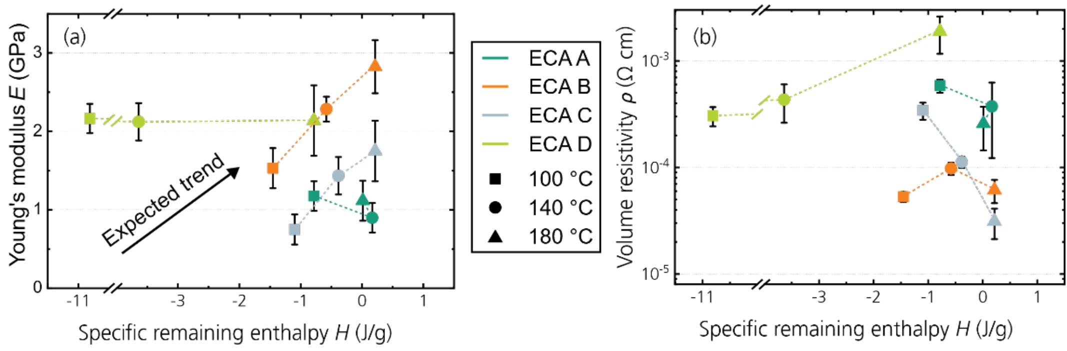

Figure 7. *Impact of incomplete curing on mechanical (T_G) and electrical (ρ) ECA properties*

4. Conclusions

In conclusion, this study investigated the influence of low curing temperatures on electrically conductive adhesives (ECAs), targeting the interconnection of perovskite-silicon tandem (PVST) solar cells. The mechanical and electrical properties of four commercially available ECAs were characterized at perovskite-compatible curing temperatures of 100 °C, 140 °C, and 180 °C as reference.

Mechanical characterization revealed diverse responses to curing temperatures: some ECAs showed increased stiffness with higher curing temperatures, while others exhibited no significant change. The glass transition temperatures (T_G) varied among the ECAs, with ECA D exhibiting significantly lower T_G when cured at 100° C, indicating incomplete curing. Electrical characterization demonstrated that lower curing temperatures were generally beneficial for lower volume resistivity, particularly for ECA C. However, joint resistance values showed high standard deviations, complicating definitive conclusions.

Void analysis indicated that void formation had a negligible effect on the mechanical properties of ECAs. Additionally, the degree of curing was found to influence mechanical properties, such as Young's modulus *E*, and electrical properties, such as volume resistivity *ρ*.

Overall, this study provides valuable insights into the relationship between curing temperature and the mechanical and electrical properties of ECAs, which is essential for the development of reliable and efficient interconnections joints. Further research in this area is crucial for optimizing the interconnection process and enhancing the long-term stability and performance of solar modules.

Data availability statement

Data underlying the results presented in this paper are not publicly available at this time. If data access for further use is needed, interested parties must contact the authors directly to request the data.

Author contributions

Leonhard Böck: Conceptualization, visualization, writing – original draft. Torsten Rößler: Conceptualization, supervision, writing – review and editing.

Competing interests

The authors declare that they have no competing interests.

Funding

This work has been funded by the Federal Ministry for Economic Affairs and Climate Action within the project “MoQa” (contract no. 0324172B).

References

[1] M. De Bastiani et al., “All Set for Efficient and Reliable Perovskite/Silicon Tandem Photovoltaic Modules?”, Solar RRL, vol. 6, no. 3, 2022, doi: https://doi.org/10.1002/solr.202100493
[2] A. De Rose et al., “Low-temperature metallization & interconnection for silicon heterojunction and perovskite silicon tandem solar cells”, SOLMAT, vol. 261, 2023, doi: https://doi.org/ 10.1016/j.solmat.2023.112515
[3] M. Pander, S. Schulze, and M. Ebert, “Mechanical Modelling of Electrically Conductive Adhesives for Photovoltaic Applications”, EU PVSEC Proceedings, pp. 3399–3405, 2014, doi: https://doi.org/ 10.4229/EUPVSEC20142014-5DV.3.39
[4] M. I. Devoto et al., “Measuring the Contact Resistivity of ECA-Based Joints”, EUPVSEC Proceedings, pp. 1001–1008, 2020, doi: 10.4229/EUPVSEC20202020-4AV.1.26
[5] V. Nikitina, et al., “High-Speed characterization of electrically conductive adhesives for industrial SHJ solar cell interconnection”, in Metallization and Interconnection Workshop Proceedings, 2022, doi: https://doi.org/ 10.1063/5.0127583
[6] N. Abdel Latif et al., “Characterization of Mechanical Strength of Shingle Joints Using Die Shear,” in SiliconPV Proceedings”, doi: https://doi.org/10.52825/siliconpv.v1i.944
[7] G. Beaucarne, “Materials Challenge for Shingled Cells Interconnection”, Energy Procedia, vol. 98, pp. 115-124, doi: https://doi.org/10.1016/j.egypro.2016.10.087
[8] A. Dhouib and S. Filali, “Operating Temperatures of Photovoltaic Modules”, in Energy and the Environment, Oxford, England: Pergamon, 1990, pp. 494-498, doi: https://doi.org/10.1016/B978-0-08-037539-7.50085-5
[9] J. Shen et at., “A Multiresolution Transformation Rule of Material Defects”, Int. J. Damage Mech., vol. 18, no. 8, pp. 739-758, 2009, doi: https://doi.org/10.1177/1056789509346693
[10] E. Koos and N. Willenbacher, “Capillary Forces in Suspension Rheology”, Science, vol. 331, issue 6019, pp. 897-900, doi: https://doi.org/10.1126/science.1199243